

Global systematics of arc volcano position

ARISING FROM Grove, T. *et al.* *Nature* 459, 694–697 (2009)

Global systematics in the location of volcanic arcs above subduction zones^{1,2} are widely considered to be a clue to the melting processes that occur at depth, and the locations of the arcs have often been explained in terms of the release of hydrous fluids near the top of the subducting slab (see, for example, refs 3–6). Grove *et al.*⁷ conclude that arc volcano location is controlled by melting in the mantle at temperatures above the water-saturated upper-mantle solidus and below the upper limit of stability of the mineral chlorite and in particular, that the arc fronts lie directly above the shallowest point of such melt regions in the mantle. Here we show that this conclusion is incorrect because the calculated arc locations of Grove *et al.*⁷ are in error owing to the inadequate spatial resolution of their numerical models, and because the agreement that they find between predicted and observed systematics arises from a spurious correlation between calculated arc location and slab dip. A more informative conclusion to draw from their experiments is that the limits of chlorite stability (figure 1b of ref. 7) cannot explain the global systematics in the depth to the slab beneath the sharply localized arc fronts.

Grove *et al.*⁷ hypothesize that arc volcano location is controlled by melting in the mantle at pressure and temperature conditions defined as ' P, T_{melt} ' in their figure 1b. Grove *et al.*⁷ then use numerical models of subduction zones to predict arc location and its global systematics. They conclude that the agreement between their calculated systematics of arc location and observations of real subduction zones^{2,8} validates their hypothesis (figure 3 of ref. 7) but closer inspection of the shape of the P, T_{melt} region casts doubt upon this conclusion. A characteristic feature of subduction-zone models⁹ is the narrow thermal boundary layer, sub-parallel to and just above the slab surface, which contains the temperature range of P, T_{melt} ($\sim 800\text{--}850\text{ }^{\circ}\text{C}$). For all but the slowest convergence rates, this boundary layer begins close to the depth at which the slab is viscously coupled to the wedge. Hence we should expect the region enclosing P, T_{melt} to be a very thin, continuous layer above the slab, with its shallowest extent at an almost constant depth.

The results of Grove *et al.*⁷ (green squares in their figure 2) are inconsistent with this expectation, and raise the suspicion of an error in their calculations.

To locate their region of P, T_{melt} , Grove *et al.*⁷ determined which nodes of their $2.3 \times 2.3\text{-km}$ computational mesh lay within that $P\text{--}T$ range. Because those conditions occur within a boundary layer only a few kilometres thick that is inclined at an angle to the mesh, this procedure did not resolve the full extent of the P, T_{melt} region. To check their results, we calculated the temperature fields for subduction zones on a $1 \times 1\text{-km}$ grid, then resampled it to both 2.3-km resolution and to 0.25-km resolution. This was done for a range of subduction parameters and for each calculation we determined the P, T_{melt} region and its shallowest point. We found that at 2.3-km resolution, the minimum depth of P, T_{melt} ranged between about 57 and 76 km, consistent with the range found by Grove *et al.*⁷. On the $0.25 \times 0.25\text{-km}$ grid, however, the minimum depth was confined between 57 and 61 km (Fig. 1a), consistent with the expectations we describe in the preceding paragraph. At either resolution, the minimum depth of P, T_{melt} is independent of the slab dip and of the convergence rate.

Grove *et al.*⁷ compare their calculations with seismic studies, which show that the depth of the slab beneath arcs varies between ~ 80 and ~ 150 km (refs 2, 8) and has a negative correlation with the descent speed of the slab (Fig. 1b). The depth to the top of the slab predicted by the hypothesis of Grove *et al.*⁷ applied under our recalculations is $\sim 60\text{--}75$ km, independent of dip or convergence rate (Fig. 1b), and thus does not agree with the observations.

The agreement between model and observations in Grove *et al.*⁷ is spurious, and is the result of their choice of variables. Figure 1c recreates their figure 3, which shows the apparent consistency between model and observations, using our recalculated location of arcs. The sine of slab dip is plotted on the x axis, and on the y axis is the arc-trench distance, which for all points (calculated and observed; see

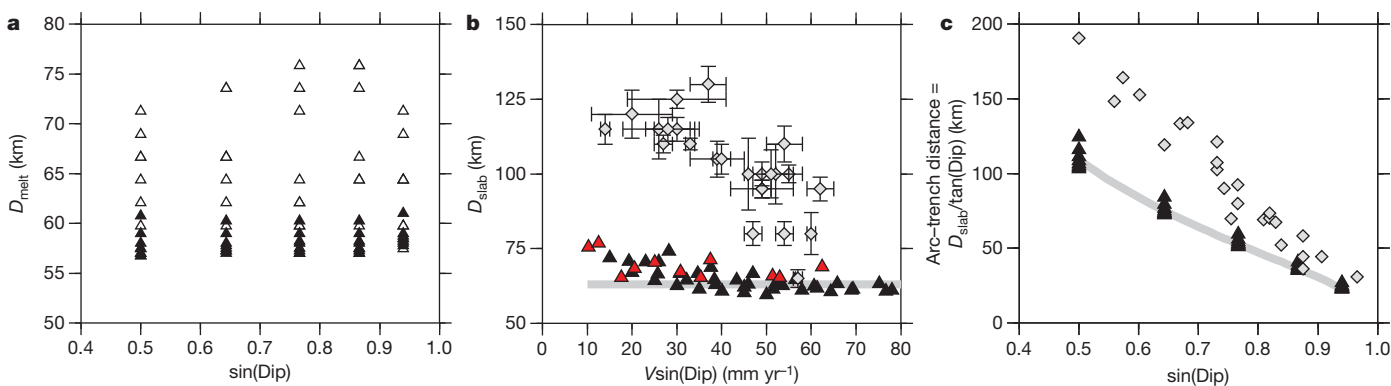


Figure 1 | Arc position versus subduction parameters for data and models. **a**, Calculated depth D_{melt} of the shallowest portion of the P, T_{melt} -based melting field (compare figures 1 and 2 of ref. 7). Calculations were carried out on a 1-km finite-volume mesh⁹, for dip of 30° to 70° in steps of 10° , and for convergence rate V from 30 to 100 mm yr^{-1} , in steps of 10 mm yr^{-1} ; these ranges include the parameters of the calculations of ref. 7. The points correspond to the minimum depths of melting calculated according to the hypothesis and methods of Grove *et al.*⁷ for a $2.3 \times 2.3\text{-km}$ resampled grid (open triangles) and for a $0.25 \times 0.25\text{-km}$ resampled grid (filled triangles). **b**, Diamonds show the depth of the slab D_{slab} , determined seismologically² (error bars as described by ref. 2); filled

triangles show the calculated D_{slab} below the locus of shallowest melting, for the $0.25 \times 0.25\text{-km}$ resampled grid from panel **a**. The red triangles correspond to the corrected values of D_{slab} for the combinations of dip and convergence rate used by ref. 7 (T. Grove *et al.*, personal communication). The grey line corresponds to a constant $D_{\text{slab}} = 62$ km. **c**, This panel corresponds to the lower 200 km of figure 3 in ref. 7. Points as for panel **b**, plotted for the horizontal distance between the trench and the arc, which is equal to $D_{\text{slab}}/\tan(\text{Dip})$, the quantity on the y axis of figure 3 of ref. 7. The grey line corresponds to $D_{\text{slab}} = 62$ km and demonstrates the spurious correlation referred to in the main text.

table 1 in ref. 7) is taken as the depth of the slab divided by the tangent of the dip. The presence of the sine of the dip on each axis ensures a spurious correlation; this is illustrated clearly in Fig. 1c by the grey line that corresponds to a constant value of the depth of the slab, $D_{\text{slab}} = 62$ km.

Therefore there is no significance in the match between models and observations reported by Grove *et al.*⁷, and their conclusion that “the kinematic control on the location of mantle melting is primarily slab dip” (page 696 of ref. 7) is mistaken. Instead, we conclude from their experiments that the limits of chlorite stability (figure 1b of ref. 7) cannot explain the global systematics in the depth of the slab beneath sharply localized arc fronts, which is true for any strongly temperature-dependent process that takes place near the top of the slab, as we have discussed. In ref. 10 we suggest a process that can account for the global systematics in location of the arcs.

Philip C. England¹ & Richard F. Katz¹

¹Department of Earth Sciences, Parks Road, Oxford OX1 3PR, UK.
e-mail: philip.england@earth.ox.ac.uk

Grove *et al.* reply

REPLYING TO England, P. C. & Katz, R. F. *Nature* **468**, doi:10.1038/nature09154 (2010)

In their Comment England and Katz¹ suggest that our model² contains two flaws and that there are additional problems in our thermal models. This Reply points out an important part of our model that England and Katz¹ appear to have missed, addresses their suggestion that there are flaws and discusses whether our thermal models are in error.

The Comment¹ states that we “conclude that the arc fronts lie directly above the shallowest point [that satisfies the P , T_{melt} criterion] in the mantle”. This corresponds to our path A in figure 1 of ref. 2. The P , T_{melt} criterion described in ref. 1 refers to the melting that initiates just above the slab over a range of depths, illustrated between paths A and C in figure 1 of ref. 2. As we discussed², when these initial melts ascend into the overlying mantle wedge, not all of them will experience a pressure–temperature path that allows them to erupt from an arc volcano on the Earth’s surface. The melts formed at the shallowest depths (path A) will encounter cooler mantle as they ascend into the overlying mantle wedge and these melts will freeze. Only melts that ascend into the hottest interior portion of the mantle wedge (such as path B in figure 1 of ref. 2) will undergo sufficient melting to produce arc front volcanoes. To summarize our findings², there are two important factors that control the location of arc volcanoes: (1) chlorite dehydration releases H₂O near the slab–wedge interface, and the H₂O ascends into overlying mantle that is above the H₂O-saturated mantle solidus (P , T_{melt} in figure 1b of ref. 2) and (2) the temperature of the overlying mantle wedge increases with decreasing pressure to allow flux melting to continue to high extents and allow these high-extent melts to erupt at arc volcanoes (path B in figure 1 of ref. 2).

England and Katz also state that the agreement that we² “find between predicted and observed systematics arises from a spurious correlation between calculated arc location and slab dip” (ref. 1). They attribute this purported spurious correlation in our figure 3 (ref. 2) to the presence of the tangent function on the vertical axis and a sine function on the horizontal axis. Although there is trigonometry involved in the correlation shown on this figure², the relations are

Received 7 September 2009; accepted 12 April 2010.

1. Tovish, A. & Schubert, G. Island arc curvature, velocity of convergence and angle of subduction. *Geophys. Res. Lett.* **5**, 329–332 (1978).
2. England, P., Engdahl, R. & Thatcher, W. Systematic variation in the depths of slabs beneath arc volcanoes. *Geophys. J. Int.* **156**, 377–408 (2004).
3. Gill, J. *Orogenic Andesites and Plate Tectonics* (Springer, 1981).
4. Tatsumi, Y. & Eggins, S. *Subduction Zone Magmatism* (Blackwell Science, 1995).
5. Iwamori, H. Transportation of H₂O and melting in subduction zones. *Earth Planet. Sci. Lett.* **160**, 65–80 (1998).
6. Tatsumi, Y. The subduction factory: how it operates in the evolving Earth. *GSA Today* **15**, 4–10 (2005).
7. Grove, T., Till, C., Lev, E., Chatterjee, N. & Medard, E. Kinematic variables and water transport control the formation and location of arc volcanoes. *Nature* **459**, 694–697 (2009); erratum **460**, 1044 (2009).
8. Syracuse, E. & Abers, G. Global compilation of variations in slab depth beneath arc volcanoes and implications. *Geochem. Geophys. Geosyst.* **7**, Q05017, doi:10.1029/2005GC001045 (2006).
9. van Keken, P. *et al.* A community benchmark for subduction zone modeling. *Phys. Earth Planet. Inter.* **171**, 187–197 (2008).
10. England, P. C. & Katz, R. F. Melting above the anhydrous solidus controls the location of volcanic arcs. *Nature* **467**, 700–703 (2010).

Competing financial interests: declared none.

doi:10.1038/nature09154

not spurious and are meaningful. The salient point in our figure 3 is that the beginning of H₂O-saturated melting in our modelling (path A in figure 1a of ref. 2) consistently occurs at a depth of 60–70 km near the slab–wedge interface and is independent of the convergence rate and dip. We point out that these shallowest melts do not reach the surface (figure 1 of ref. 2), nor do they influence the location of volcanoes. Instead, the maximum amount of melting and hence the location of arc volcanoes are controlled by the position of the hottest part of the wedge above a slab. This is the region between paths B and C (figure 1 of ref. 2), the region of maximum melting from our models. The arc–trench distance for paths B to C, and thus the location of arc volcanoes, is close to the values reported by England *et al.*³ and parallel to the trend of Syracuse and Abers⁴. The distance a given isotherm is from the trench decreases with increasing convergence rate and spans a range of values that are represented in the data of ref. 3. An interesting outcome of our thermal modelling (figure 2 of ref. 2) is that at steep dip angles, paths A and B occur at very similar distances from the trench.

England and Katz say that our thermal modelling results (in figure 2 of ref. 2) “raise the suspicion of an error in [our] calculations” (ref. 1). England and Katz continue with a discussion of grid size in the numerical calculations that they performed, but it is impossible for us or for any reader of the Comment¹ to assess the veracity of their claim that we² “did not resolve the full extent of the P , T_{melt} region” (ref. 1). We have verified our modelling methods using the community benchmarks developed for subduction zone modelling⁵ and we also find that our model results for the temperature structure near the slab–wedge interface are comparable to those of others who have benchmarked their models, such as Wada and Wang⁶, who explicitly considered the issues associated with slab–mantle viscous coupling.

Thus, we disagree with the conclusion reached by England and Katz¹ that “the limits of chlorite stability cannot explain the global systematics in the depth of the slab beneath sharply localized arc fronts”. The conclusions we reached in ref. 2 rely on the interplay

BRIEF COMMUNICATIONS ARISING

of two important controls on hydrous melting in the mantle wedge above subducted slabs: the dehydration of chlorite near the base of the wedge and the temperature structure of the overlying mantle wedge.

T. L. Grove¹, C. B. Till¹, E. Lev², N. Chatterjee¹ & E. Médard³

¹Department of Earth, Atmospheric and Planetary Sciences, Massachusetts Institute of Technology, Cambridge, Massachusetts 02139, USA.

e-mail: tlgrove@mit.edu

²Lamont-Doherty Earth Observatory, Columbia University, Palisades, New York 10964, USA.

³Laboratoire Magmas et Volcans, Université Blaise Pascal, Clermont-Ferrand, F-63038, France.

1. England, P. C. & Katz, R. F. Global systematics of arc volcano position. **468**, doi:10.1038/nature09154 (this issue).
2. Grove, T., Till, C., Lev, E., Chatterjee, N. & Médard, E. Kinematic variables and water transport control the formation and location of arc volcanoes. *Nature* **459**, 694–697 (2009); erratum **460**, 1044 (2009).
3. England, P., Engdahl, R. & Thatcher, W. Systematic variation in the depths of slabs beneath arc volcanoes. *Geophys. J. Int.* **156**, 377–408 (2004).
4. Syracuse, E. M. & Abers, G. A. Global compilation of variations in slab depth beneath arc volcanoes and implications. *Geochem. Geophys. Geosyst.* **7**, Q05017, doi: 10.1029/2005GC001045 (2006).
5. van Keken, P. E., *et al.* A community benchmark for subduction zone modeling. *Phys. Earth Planet. Inter.* **171**, 187–197 (2008).
6. Wada, I. & Wang, K. Common depth of slab-mantle decoupling: reconciling diversity and uniformity of subduction zones. *Geochem. Geophys. Geosyst.* **10**, Q10009, doi: 10.1029/2009GC002570 (2009).

doi:10.1038/nature09155